Biosensors and Bioelectronics 65 (2015) 245–250

Contents lists available at ScienceDirect

Biosensors and Bioelectronics

journal homepage: www.elsevier.com/locate/bios

A dual-amplified electrochemical detection of mRNA based on duplex-specific nuclease and bio-bar-code conjugates

Xue-Mei Li [a,*], Lin-Lin Wang [b], Jie Luo [b], Qing-Li Wei [b]

[a] School of Chemistry and Chemical Engineering, Linyi University, Linyi 276005, PR China
[b] State Key Laboratory Base of Eco-chemical Engineering, College of Chemistry and Molecular Engineering, Qingdao University of Science and Technology, Qingdao 266042, PR China

ARTICLE INFO

Article history:
Received 6 July 2014
Received in revised form
17 October 2014
Accepted 20 October 2014
Available online 23 October 2014

Keywords:
Duplex-specific nuclease
Dual-amplification
Bio-bar-code
Electrochemistry

ABSTRACT

On the basis of strong preference for cleaving double-stranded DNA or DNA in DNA:RNA heteroduplexes of duplex-specific nuclease (DSN), a dual-amplified electrochemical detection of mRNA was developed in this article, by coupling the enhancement of DSN and bio-bar-code conjugates. Capture probe was linked with magnetic nanoparticles (MNPs) at its 5′ end and bio-bar-code at its 3′ end. In the presence of target surviving mRNA, all hybridized $\mathbf{S_1}$ strands were cleaved off the biosensor by the DSN, and the bio-bar-code probe with CdS nanoparticles (CdS NPs) was released into the solution. The metal sulfide nanoparticles were measured by anodic stripping voltammetry (ASV) subsequently. This assay exhibited high sensitivity and selectivity with a detection limit of 0.48 fM. In addition, we proved that this simple and cost-effective strategy is capable of detecting the target in complicated biological samples and holds great potential application in biomedical research and clinical diagnostics.

1. Introduction

Messenger RNA (mRNA), a single-stranded ribonucleic acid, is an informational molecule. Due to their key position at the intersection between the genome and proteome, mRNA transcripts are disease-relevant and can be utilized as markers in research and medical diagnostic applications (Sunde, 2010). Tumor-related mRNA has been widely used as a specific marker to assess the migration of tumor cells locally or in the bloodstream (Schwarzenbach et al., 2011). The sensitive and selective detection of mRNAs is of great significance for a full understanding of mRNA functions and diagnosis of diseases. Recently, several methods such as electrochemistry (Stephen et al., 2008), electrochemiluminescence (Wu et al., 2012), microarray analysis (Reinholt et al., 2014), real-time polymerase chain reaction (RT-PCR) (Nolan et al., 2006) and fluorescence imaging (Qiu et al., 2013) have been developed for mRNA detection.

Typically, in situ visualization of gene expression in cells has been implemented using the fluorescence in situ hybridization (FISH) strategy (Wienholds et al., 2005; Larsson et al., 2004). However, the FISH method usually shows limited sensitivity and is not applicable to situations where RNA is expressed in very low amounts. In order to improve the sensitivity, some amplification methods have been combined with FISH, such as rolling-circle amplification (RCA)-based FISH (Larsson et al., 2010) and single-molecule imaging FISH (Buxbaum et al., 2014) have been introduced for in situ sensitive detection of mRNA expression. However, mRNA analysis using surface hybridization-based biosensors can be complicated by the size and extensive secondary structure of the full length transcript (Carrascosa et al., 2012). Therefore, more cost-effective and high sensitive biosensors for the detection of RNA have been explored, with enzymatic or other signal amplification methodologies (Ge et al., 2014; Kindt and Bailey, 2012).

Duplex specific nuclease (DSN), a nuclease isolated from hepatopancreas of the Kamchatka crab (Paralithodes camtschaticus) (Shagin et al., 2002), is known to be able to cleave DNA with a high preference in double-stranded DNA (dsDNA) or DNA in DNA:RNA heteroduplexes. Moreover, because it is practically inactive toward single-stranded DNA, or single- or double-stranded RNA, it has been used for the detection of microRNA. Very recently a new duplex-specific nuclease signal amplification (DSNSA) strategy has been developed for highly sensitive detection of miRNA by Ye's group (Yin et al., 2012). Subsequently, an increasing interest in the development of DSNSA has been presented for the detection of miRNA by fluorescent detection (Degliangeli et al., 2014; Wang et al., 2014; Li et al., 2014), and electrochemical techniques (Ren et al., 2013). Most of the reported DSNSA protocols used the single enhancement of DSN, few dual-amplified strategies have been reported (Tian et al., 2013).

* Corresponding author. Fax: +86 539 8766867.
E-mail address: xuemei_li@yeah.net (X.-M. Li).

http://dx.doi.org/10.1016/j.bios.2014.10.051
0956-5663/

The recently developed bio-bar-code assay, based on Au NPs functionalized both with oligonucleotides (the barcodes as a surrogate target) and a target recognition element, has been shown to be extraordinarily sensitive, exhibiting low attomolar sensitivity for protein targets and high zeptomolar sensitivity for nucleic acid targets (Nam et al., 2003; Stoeva et al., 2006). Herein, we reported a dual-amplified duplex-specific nuclease signal amplification (DA-DSNSA) strategy by coupling the enhancement of DSN and bio-bar-code conjugates, achieving further improvement of sensitivity.

2. Experimental section

2.1. Apparatus

All electrochemical measurements were conducted in a standard electrochemical cell using an electrochemical analyzer (CHI660E, CH Instruments, USA). The three-electrode system consists of the glassy carbon electrode (GCE, 1.0 mm diameter) as working electrode, a Pt-wire electrode as the counter electrode, and an Ag/AgCl reference electrode. Anodic stripping voltammetry was conducted with an in situ formed mercury film electrode (on a glassy carbon surface) generated as working electrode, by accumulation for 200 s at −1.2 V. After standing for 15 s, the stripping voltammetry was carried out between −0.8 V and −0.4 V at 50 mV s^{-1} under N_2 atmosphere using a square-wave voltammetry, with a frequency of 25 Hz, amplitude of 50 mV, and potential step of 4 mV.

2.2. Chemicals

All oligonucletides in the present study were purchased from SBS Genetech Co., Ltd. (Beijing, China) or Takara Biotechnology Co., Ltd (Dalian, China), and their sequences were provided in Supplementary Table S1. The DSN was supplied by Genomax Technologies Pte Ltd. (Singapore). Carboxyl-modified magnetic beads (MBs) (~1.0 μm, 10 mg/mL) were obtained from BaseLine Chrom Tech Research Centre (Tianjin, China). Magnetic beads modified with gold shell (Fe_3O_4@Au, ~50 nm, 5 mg/mL) were obtained from Xi'an GoldMag Nanobiotech Co., Ltd (Xi'an, China). 1-Ethyl-3-(3-dimethylaminopropyl)-carbodiimide hydrochloride (EDC) and *N*-hydroxysuccinimide (NHS) were purchased from Sigma-Aldrich. In order to minimize the effect of RNase on the stability of mRNA, the solutions and glassware tubes used in the DSNSA method were treated with 0.1% diethylpyrocarbonate (DEPC) and autoclaved. Other chemicals employed were all of analytical grade and triple distilled water was used throughout. Lab equiments were all soaked in aqua regia to remove contaminants and washed with triple distilled water for several times.

2.3. Preparaton of AuNPs

Gold nanoparticles were prepared by citrate reduction of $HAuCl_4$ according to the literature (Liu and Lu, 2006). Briefly, 10 mL of 38.8 mM sodium citrate was immediately added to 100 mL of 1.0 mM $HAuCl_4$ refluxing solution under stirring, and the mixture was kept boiling for another 15 min. The solution color turned to a wine red, and was cooled to room temperature with continuous stirring. The sizes of the AuNPs were verified by transmission electron micrograph (TEM) using a JEOL JEM-2100EX microscope (Japan). The AuNPs have average diameters of 20 nm (as shown in Figure S1 in the supporting information).

2.4. Preparation of CdS Nanoparticles labeled with S_2

Nanoparticles of cadmium sulfide were prepared according to our previously reported reference (Li et al., 2010). A 2 μL of mercaptoacetic acid was added to 100 mL of 1 mM of cadmium chloride solution under vigorous stirring, and the pH was adjusted to 11 with 0.5 M NaOH. The solution was bubbled with nitrogen for 30 min, and 50 mL of 1.34 mM Na_2S was added dropwise to the solution. The reaction was kept for 24 h under bubbling nitrogen.

A 200 μL of 0.1 M imidazole solution (pH 7.0) was added to 1.0 mL of the prepared CdS NPs solution. After 30 min, 100 μL of 0.1 M EDC solution and 1.8×10^{-10} mol of $\mathbf{S_2}$ were added to the mixture and incubated at room temperature for 24 h with gentle shaking. Excess reagents were removed by centrifugation at 10,000 rpm for 30 min. The precipitate was washed and then dispersed 200 μL PBS solution. The solution of $\mathbf{S_2}$-modified CdS NPs was stored at 4 °C for the hybridizations and kept stable for several weeks. The resulting nanoparticles have average diameters of 10 nm as characterized by TEM (Figure S1).

2.5. Preparation of S_1-immobilized MBs

A 50 μL suspension of carboxyl MNPs (10 mg mL^{-1}) was washed three times with 0.1 M imidazol–HCl buffer (pH 7.0, 3 × 100 μL). A 0.1 M EDC solution (100 μL) was added to the MB solution and the mixture was incubated at room temperature for 20 min to activate the carboxylate groups on the MNPs. Then, 1.8×10^{-10} mol $\mathbf{S_1}$ was added and the resulting mixture was stirred for 1 h. After magnetic separation, MNPs were washed three times with 0.1 M PBS buffer. The washed MNP/$\mathbf{S_1}$ resuspended in 200 μL PBS solution was stored at 4 °C for further use and kept stable for several weeks. The surface coverage of $\mathbf{S_1}$ on MNPs was determined according to UV–visible absorbance (Fig. S2 in the supporting information).

2.6. Fabrication of MNPs-S_1-AuNPs-S_2-CdS NPs sensing system

The fabrication of MNPs-$\mathbf{S_1}$-AuNPs-$\mathbf{S_2}$-CdS NPs was carried out based on a slightly modified literature protocol (Zhang et al., 2008a). Briefly, the mixture of 200 μL of prepared MNP-$\mathbf{S_1}$ and 200 μL of prepared $\mathbf{S_2}$-CdS NPs was activated with acetate buffer (pH 5.2) and 5 μL of 10 mM TCEP for 1 h, and then added to 1 mL of freshly prepared AuNPs and shaken gently overnight. After reaction of 16 h, the DNA–AuNP conjugates were aged in salts (0.01 M NaCl, 5.0 mM tris-acetate buffer) for another 40 h. Excess reagents were removed by centrifuging at 15,000 rpm for 30 min. The red precipitate was washed, recentrifuged, and dispersed in 1 mL of buffer containing 300 mM NaCl, 25 mM tris(hydroxymethyl)aminomethane (Tris) acetate, pH 8.2. The solution of the prepared probe was stored at 4 °C and kept stable for several weeks. The MNPs modified with AuNPs and CdS NPs were characterized by TEM (Fig. S1).

2.7. Detection of target mRNA

A volume of 30 μL reaction mixture containing 1 × DSN buffer (50 mM Tris–HCl, pH 8.0; 5 mM $MgCl_2$, 1 mM DTT), 0.2 U DSN (dissolved in 25 mM Tris–HCl, pH 8.0; 50% glycerol), MNPs-$\mathbf{S_1}$-AuNPs-$\mathbf{S_2}$-CdS NPs conjugates and mRNA target, was incubated in a thermal cycler at 60 °C for 40 min. Subsequently, the reaction mixture was added 30 μL 10 mM EDTA and incubated at 60 °C for 5 min to inactive DSN enzyme. After magnetic separation, the supernatant was treated with a solution of 150 μL 0.2 M HNO_3 for 10 min. The solution containing the dissolved quantum dots were transferred into 2 mL of acetate buffer (0.10 M,

pH=5.3) containing 0.01 g/L of mercury ions and ASV was conducted.

2.8. Cell culture and preparation of extracts

Human cervical cancer cell lines (HeLa) and Jurkat cell lines were cultured in RPMI 1640 medium supplemented with 10% fetal bovine serum (FBS) and 100 IU/mL penicillin streptomycin and the cells were harvested by trypsinization. The cell density was determined by using a hemocytometer prior to any experiments. Approximately one million cells dispersed in RPMI 1640 cell media buffer were centrifuged at 3000 rpm for 5 min and rinsed wit 5 mL of dye-free cell media three times and were then redispersed in cell media buffer (1 mL). Finally, the cells were disrupted by sonication for 20 min at 0 °C. To remove the homogenate of cell debris, the lysate was centrifuged at 18 000 rpm for 20 min at 4 °C.

3. Results and discussion

3.1. Fabrication of sensing system based on DSN amplification

Scheme 1 depicts the working principle of the label-free electrochemical biosensor for mRNAs. The system consists two kinds of DNA sequences, both of which were labeled with $-NH_2$ at 5′ end and –SH at 3′ end. The 3′-thiolmodified **S_1** and **S_2** were loaded on the AuNP surface via sulfur–gold affinity. The amine-modified **S_1** and **S_2** were linked with carboxyl MNPs and CdS NPs, respectively, via amino bond. Thus, the MNPs-**S_1**-AuNPs-**S_2**-CdS NPs sensing system was fabricated. In the presence of target mRNA, DNA–mRNA (**S_1**-mRNA) heteroduplexes were formed (see Fig. S3 in the supporting information). All hybridized **S_1** strands were cleaved off the biosensor by the DSN. It has been demonstrated that the DSN selectively cleaves double stranded DNA (dsDNA) and DNA – RNA duplexes with little activity toward single-stranded nucleic acids and RNA – RNA duplexes (Ren et al., 2013). As a result, the AuNPs together with CdS NPs were released into the solution. Since there are more than 100 CdS NPs loading on one AuNP (Zhang et al., 2008b), the sensitivity of the assay was greatly enhanced. Concurrently, the released target mRNA strands are recycled for further hybridization, forming an isothermal signal amplification cycle. This cyclic reaction generates a great amplification of electrochemical signal. The nanoparticles in the solution were dissolved with a solution of HNO_3 for 20 min and were determined by stripping voltammetry.

3.2. Optimization of the incubation

To demonstrate the working principle of the bio-bar-code assisted DSNSA method, we selected survivin mRNA as a model to optimize the experimental conditions. The antisense oligonucleotide portion of the nanoconjugate targets an mRNA region selected to control expression of survivin, a well-studied gene used in cancer diagnosis and treatment (Fukuda and Pelus, 2006).

There is only one enzyme used in the present work, the working temperature of the DSN was fixed at its optimal temperature of 50 °C to ensure the amplification power of DSN for sensitivity enhancement (Xi et al., 2014). It has been previously reported that DSN is stable at a wide range of pH (from 4 to 12) in the presence of 5 mM Mg^{2+} (Yin et al., 2012). The pH value was set as 8.0. In order to achieve the best assay performance, the amplification and sensing conditions including the working time and the amount of DSN were investigated. As shown in Fig. 1A in the supporting information, a peak current increased immediately when the DSN was introduced and then tended to stabilize after more than 40 min. Thus 40 min was chosen as the reaction time in whole experiments. Subsequently, we optimized the amount of DSN. An optimal electrochemical difference in the presence and absence of mRNA was observed when DSN was 0.2 U in a 30 μL reaction mixture (Fig. 1B). Hence, 0.2 U of DSN was used throughout subsequent experiments.

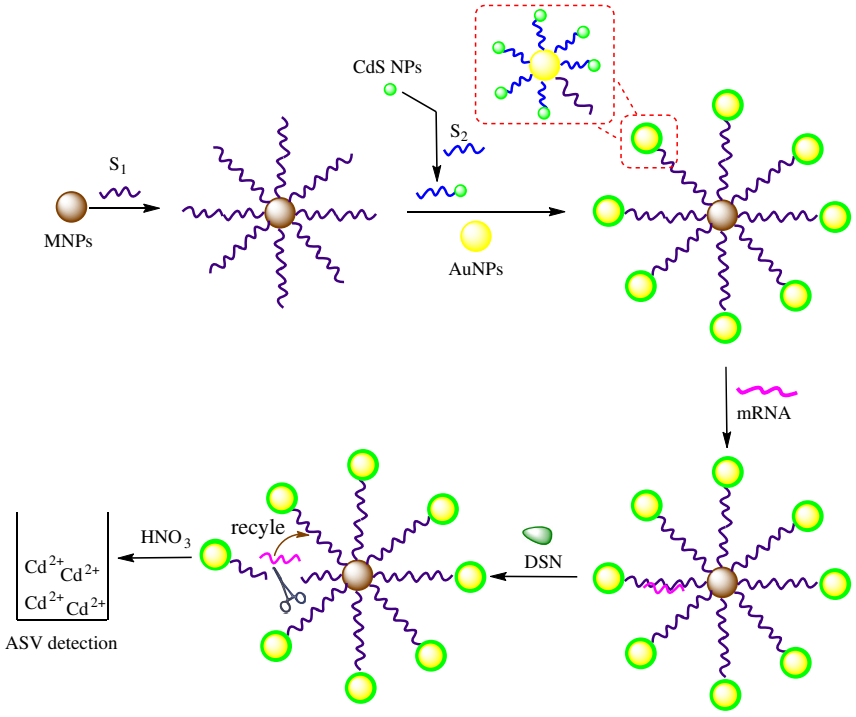

Scheme 1. Schematic representation of the sensing interface for the label-free electrochemical detection of mRNA with dual-amplification of DSN and bio-bar-code.

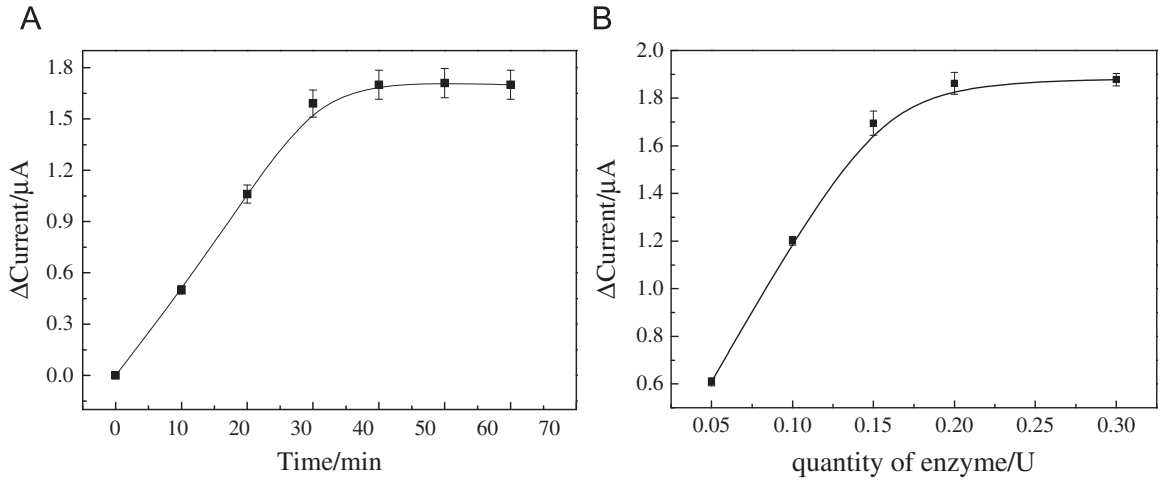

Fig. 1. Effect of reaction time (A) and concentration of DSN (B) on electrochemical intensity. The concentration of mRNA was 10 pM for both. Error bars are the standard deviation of three repetitive experiments.

3.3. *Effect of the dual-amplification*

To prove the dual amplification effect by DSN and bio-bar-code conjugates, the control experimental without the bio-bar-code was carried out as shown in Scheme S1 in the supporting information. It could be seen from Fig. S4 that this strategy only showed a detection limit of about 1 pM for target mRNA.

In addition, to investigate the signal amplification effect of the DSN, the DNA target with the same base sequences was determined through the present dual-amplified strategy. DSN displays a strong preference for cleaving double-stranded DNA or DNA in DNA:RNA heteroduplexes, and is practically inactive toward single-stranded DNA (Shagin et al., 2002). When target DNA was hybridized with capture DNA $\mathbf{S_1}$, both are cleaved by DSN. Thus the target DNA cannot recycle and the amplification of DSN was inhibited as a result. As shown in Fig. 2, the electrochemical responses to target mRNA at the same concentration was significantly higher than that of DNA. The peak currents for the mRNA was about 5 times higher than that for DNA, showing the remarkable amplification performance of DSN.

3.4. *Sensitive detection of mRNA*

Under the optimum conditions, the sensitivity of the DSNSA method was investigated upon addition of different concentrations of mRNA. Fig. 3 showed the ASV response for the dissolved

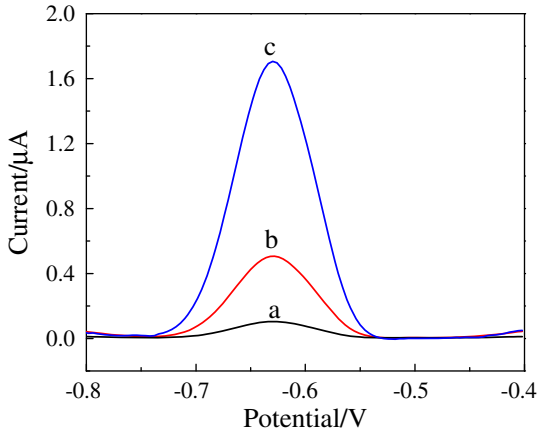

Fig. 2. ASV response of (a) base line, (b) DNA and (c) mRNA. The concentration of target was both 1.0 pM.

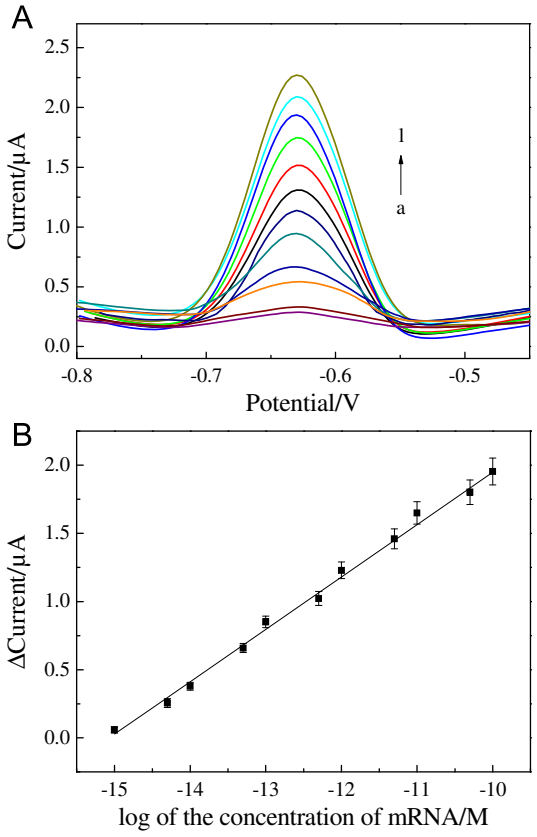

Fig. 3. (A) Anodic stripping voltammetry analysis of the CdS nanoparticles in the solution after treatment with surviving mRNA. Concentrations of surviving mRNA: 0, 1.0 fM, 5.0 fM, 10 fM, 50 fM, 100 fM, 500 fM, 1.0 pM, 5.0 pM, 10 pM, 50 pM, 100 pM. (B) The linear relationship between the peak current and the concentration of surviving mRNA. Error bars are the standard deviation of three repetitive experiments.

CdS after different concentrations of mRNA was introduced (the concentrations of Cd^{2+} were investigated in Fig. S5 in the supporting information). From the ASV response, one could see that the response to sample mixtures increased with the increasing levels of the target mRNA. mRNA could be quantified over a concentration range from 1.0×10^{-15} M to 1.0×10^{-10} M. The regression equation was $y=5.85555+0.38897$ lg X (y was the Δi, μA; X was the concentration of mRNA, M), and the regression coefficient of the linear curve was $R^2=0.9955$. A detection limit of

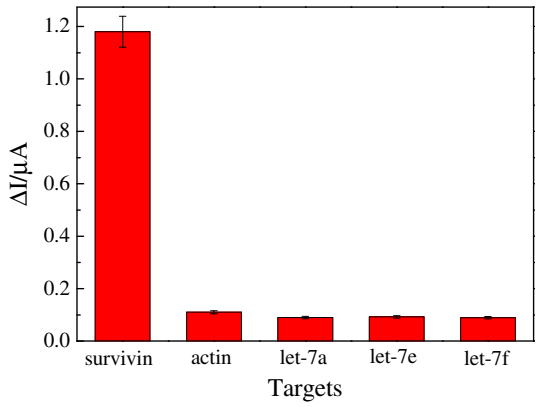

Fig. 4. Specificity of mRNA assay. Bars represent the electrochemical intensity difference (I–I_0) upon the different RNAs targets (1.0 pM for surviving mRNA and 10 pM for others), where I and I_0 are the electrochemical signals in the absence and the presence of target RNA, respectively. Error bars are the standard deviation of three repetitive experiments.

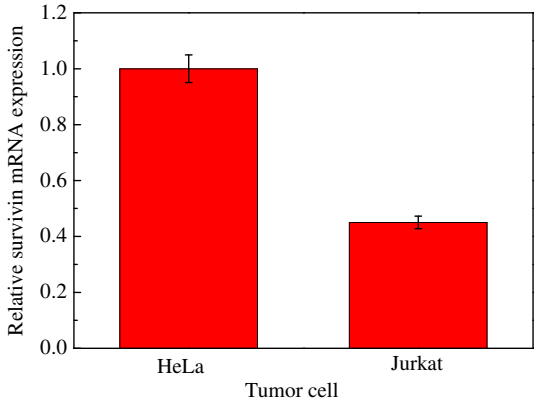

Fig. 5. Detection of survivin mRNA expression levels in different cell lysate. Error bars are standard deviation of three repetitive experiments.

4.8×10^{-16} M of surviving mRNA can be estimated using 3σ, which is more than 2 orders of magnitude lower than that of basic DSNSA (1.0 pM), and is more lower than the previously reported electrochemical RNA detection with DSN assays (Ren et al., 2013). The amplification of the present protocol was mainly ascribed to the bio-bar-code technology that can efficiently avoid cross-reaction. Moreover, the highly sensitive response of the DSN for mRNA detection also exhibited satisfactory reproducibility. The standard deviations of eight duplicated tests at 10 fM and 10 pM were found to be ~12% and ~8%, respectively.

3.5. Selectivity of the sensing strategy

The capability in discriminating closely related RNAs in a RNA family is pretty important for their further applications in diagnostic study. Next, we further assessed the anti-interference properties of our newly developed strategies, by treating with solutions containing different RNA targets. Actin mRNA and three representative members of let-7 family were selected to evaluate the specificity of the biosensor. As can be seen from Fig. 4, even with concentrations as high as 1.0×10^{-11} M of actin mRNA, let-7a, let-7e and let-7f, signals were not more than 10% relative to those toward the case of target survivin mRNA. This high specificity is much better than those of previously reported mRNA biosensors (Li et al., 2012), due to the mismatch discrimination ability of the DSN (Table S2).

3.6. Application of the sensor in biological sample

Inspired by the high sensitivity and selectivity, we examined the performance of the detection of mRNA in complicated biological samples. In this case, analysis of cellular survirin mRNA from lysates of HeLa cell with relatively high levels of survivin and Jurkat cell with relatively low levels was carried out (Prigodich et al., 2012). Consistent with the known literature, a comparatively higher expression level of surviving mRNA in Hela cell lines than Jurkat cell lines could be observed with the present protocol as shown in Fig. 5. The application in the cell lysates showed good feasibility (Fig. S6 in the supporting information).

4. Conclusion

In summary, by taking advantages of DSN and bio-bar-code probes, we developed a dual-amplified electrochemical strategy, and demonstrated its application for rapid ultrasensitive detection of mRNA. As compared to other mRNA assays, the proposed electrochemical biosensor exhibited several distinct advantages: freedom from thermal amplification and excellent sensitivity. Because the DSN is specific to RNA and has no special requirements on the nucleic sequence, the assay strategy is general enough to be extended to the parallel quantification of a selected panel of RNAs, such as microRNA, siRNA, etc. The simultaneous detection and quantification of multiple mRNAs is feasible by use of different metal – oxide semiconductors.

Acknowledgments

This work was supported by the National Natural Science Foundation of China (No. 21275083) and the Scientific and Technical Development Project of Linyi (201312023).

Appendix A. Supporting Information

Supporting information associated with this article can be found in the online version at.

References

Buxbaum, A.R., Wu, B., Singer, R.H., 2014. Science 343, 419–422.
Carrascosa, L.G., Gomez-Montes, S., Avino, A., Nadal, A., Pla, M., Eritja, R., Lechuga, L. M., 2012. Nucleic Acids Res. 40, e56.
Degliangeli, F., Kshirsagar, P., Brunetti, V., Pompa, P.P., Fiammengo, R., 2014. J. Am. Chem. Soc. 136, 2264–2267.
Fukuda, S., Pelus, L.M., 2006. Mol. Cancer Ther. 5, 1087–1098.
Ge, J., Zhang, L.L., Liu, S.J., Yu, R.Q., Chu, X., 2014. Anal. Chem. 86, 1808–1815.
Kindt, J.T., Bailey, R.C., 2012. Anal. Chem. 84, 8067–8074.
Larsson, C., Grundberg, I., Soderberg, O., Nilsson, M., 2010. Nat. Methods. 7, 395–397.
Larsson, C., Koch, J., Nygren, A., Janssen, G., Raap, A.K., Landegren, U., Nilsson, M., 2004. Nat. Methods 1, 227–232.
Li, N., Chang, C.Y., Pan, W., Tang, B., 2012. Angew. Chem. Int. Ed. 51, 7426–7430.
Li, X.M., Liu, J.M., Zhang, S.S., 2010. Chem. Commun. 46, 595–597.
Li, X.L., Wang, Y.C., Zhang, X.J., Zhao, Y.J., Liu, C.H., Li, Z.P., 2014. Acta Chim. Sin. 72, 395–400.
Liu, J., Lu, Y., 2006. Nat. Protoc. 1, 246–252.
Nam, J.M., Thaxton, C.S., Mirkin, C.A., 2003. Science 301, 1884–1886.
Nolan, T., Hands, R.E., Bustin, S.A., 2006. Nat. Protoc. 1, 1559–1582.
Prigodich, A.E., Randeria, P.S., Briley, W.E., Kim, N.J., Daniel, W.L., Giljohann, D.A., Mirkin, C.A., 2012. Anal. Chem. 84, 2062–2066.
Qiu, L.P., Wu, C.C., You, M.X., Han, D., Chen, T., Zhu, G.Z., Jiang, J.H., Yu, R.Q., Tan, W. H., 2013. J. Am. Chem. Soc. 135, 12952–12955.
Reinholt, S.J., Behrent, A., Greene, C., Kalfe, A., Baeumner, A.J., 2014. Anal. Chem. 86, 849–856.
Ren, Y.Q., Deng, H.M., Shen, W., Gao, Z.Q., 2013. Anal. Chem. 85, 4784–4789.
Schwarzenbach, H., Hoon, D.S.B., Pantel, K., 2011. Nat. Rev. Cancer 11, 426–437.

Shagin, D.A., Rebrikov, D.V., Kozhemyako, V.B., Altshuler, I.M., Shcheglov, A.S., Zhulidov, P.A., Bogdanova, E.A., Staroverov, D.B., Rasskazov, V.A., Lukyanov, S., 2002. Genome Res. 12, 1935–1942.
Stephen, S.W., Yeung, T.M.H.L., Hsing, I.M., 2008. Anal. Chem. 80, 363–368.
Stoeva, S.I., Lee, J.S., Smith, J.E., Rosen, S.T., Mirkin, C.A., 2006. J. Am. Chem. Soc. 128, 8378–8379.
Sunde, R.A., 2010. J. Nutr. Biochem. 21, 665–670.
Tian, T., Xiao, H., Zhang, Z.G., Long, Y.L., Peng, S., Wang, S.R., Zhou, X., Liu, S.M., Zhou, X., 2013. Chem. Eur. J 19, 92–95.
Wang, S.R., Fu, B.S., Wang, J.Q., Long, Y.L., Zhang, X.E., Peng, S., Guo, P., Tian, T., Zhou, X., 2014. Anal. Chem. 86, 2925–2930.
Wienholds, E., Kloosterman, W.P., Miska, E., Alvarez-Saavedra, E., Berezikov, E., Bruijn, D.E., Horvitz, H.R., Kauppinen, S., Plasterk, R.H., 2005. Science 309, 310–311.
Wu, M.S., Qian, G.S., Xu, J.J., Chen, H.Y., 2012. Anal. Chem. 84, 5407–5414.
Xi, Q., Zhou, D.M., Kan, Y.Y., Ge, J., Wu, Z.K., Yu, R.Q., Jiang, J.H., 2014. Anal. Chem. 86, 1361–1365.
Yin, B.C., Liu, Y.Q., Ye, B.C., 2012. J. Am. Chem. Soc. 134, 5064–5067.
Zhang, S., Xia, J., Li, X., 2008a. Anal. Chem. 80, 8382–8388.
Zhang, S., Zhong, H., Ding, C., 2008b. Anal. Chem. 80, 7206–7212.